Electrostatically-Tunable Analog RF MEMS Varactors with Measured Capacitance Range of 300%

Dimitrios Peroulis[1] and Linda P. B. Katehi[2]
[1]Radiation Laboratory, Electrical Engineering and Computer Science Department, University of Michigan, Ann Arbor, MI 48109-2122.
[2]School of Electrical and Computer Engineering, Purdue University, West Lafayette, IN 47907-1280.
dperouli@umich.edu, katehi@purdue.edu

Abstract— **This paper reports on the design, fabrication, and testing of a novel analog MEMS varactor with measured tuning range of 300%. The proposed electrostatically actuated varactor is based on a parallel-plate approach and is best suited for microwave/millimeter-wave applications. The measured capacitance values are in the range of 40–160 fF and are achieved with DC voltages of 20-34 V. The proposed varactor has the additional advantages of very high resonant frequency (its series measured parasitic inductance is 9 pH) and high quality factor (higher than 80 at 40 GHz).**

I. Introduction

NUMEROUS high-frequency MEMS switches have been recently demonstrated [1] with outstanding RF performance and typical capacitance ratios in the range of 70:1. The majority of these designs rely on electrostatic actuation because of its simplicity and its very low biasing power requirements. This actuation mechanism results in the well-known pull-in effect that forces the micro-switch to collapse when it moves one third of its initial height. Although this effect does not significantly impair the switching operation, it can be a serious limitation to MEMS variable capacitors, if a similar actuation mechanism is followed.

Two main approaches have been proposed in the literature to overcome this issue: 1) digital varactors by using a bank of MEMS switches [2] and 2) extended tuning range analog variable capacitors [3], [4], [5]. Digital designs can provide high tuning ranges, but the interconnects between the individual switches typically require a significant amount of space and considerably limit their bandwidth. Although these limitations do not apply to the analog designs, the reported analog extended range parallel-plate MEMS varactors have shown limited tuning range (in the order of 50-70%) mostly because due to residual stress that limits the theoretically expected capacitive range.

Our proposed varactor also follows the extended tuning range approach, but it is based on a two-metal, two-sacrificial-layer process and results in a measured tuning range of nearly 300%. This varactor design is also very robust to residual stress and is presented in Section II. The fabrication process follows in Section III, while our experimental results are discussed in Section IV.

II. RF MEMS Capacitor Design

Fig. 1a shows a schematic of the proposed device. This device is composed of two Au beams. The first beam (lower beam) is a 0.7-μm thick beam that is suspended $g_1 = 2$ μm above a 50/80/50-μm coplanar waveguide (cpw) line, while the second one (upper beam) is 13-μm thick and is suspended $g_2 = 6$ μm above the lower beam. Figs. 1b and c illustrate two possible implementations of the lower beam. The first one (Fig. 1b) shows a folded-suspension lower beam design (FSLB design), while the second one (Fig. 1c) shows a fixed-fixed lower beam design (FFLB design). The second difference between the two implementations is the fact that in the FSLB design a dielectric layer covering the cpw line prevents direct metal contact between the lower beam and the center conductor of the cpw, while this is not the case in the FFLB design. Both implementations are based on the same design principles but they yielded slightly different experimental results, which are presented and compared in Section IV.

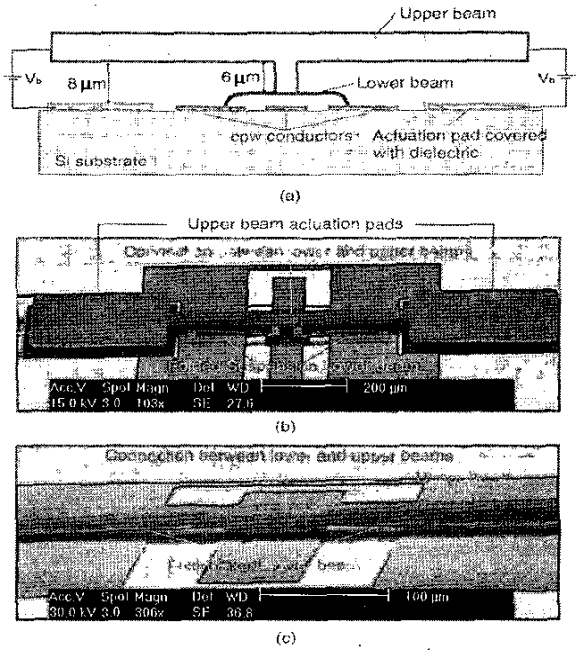

Fig. 1. (a) Schematic diagram of the proposed analog MEMS varactor. (b) First implementation of the analog MEMS varactor. This varactor uses a folded-suspension lower beam (FSLB) and a dielectric layer underneath the lower beam. (c) Second implementation of the analog MEMS varactor This varactor uses a fixed-fixed lower beam (FFLB) and it does not have any dielectric layer that could prevent a DC-contact between the lower beam and the center conductor of the cpw.

0-7803-7695-1/03/$17.00 © 2003 IEEE

In both designs the anchor points of the lower beam are connected to the ground planes of the cpw line. Furthermore, in both designs the upper beam (which is suspended $g_2 = 6$ μm above the lower beam) has no anchor points, but is connected to the middle of the lower beam. Although the upper beam is almost 1-mm long, it is very stiff, because it is made of 13 μm of low-stress electroplated Au. The upper beam also forms two 360×300-μm^2 pads (upper pads) that are suspended a total distance of $g_{tot} = g_1 + g_2 = 8$ μm above the two electrostatic actuation pads covered with a dielectric layer as shown in Fig. 1a.

When an electrostatic potential V_b is applied between the upper beam and the two actuation pads, the lower beam deflects, because its spring constant is three orders of magnitude lower than the upper beam's. Additionally, because of the height difference between the two beams, the pull-in instability for the upper beam does not occur until it moves by approximately 2.5 μm downwards. This means that the upper beam does not collapse before the lower beam touches the center conductor of the cpw line (in the FFLB case) or the dielectric layer covering it (in the FSLB case). When this happens (at $V_b = V_{ct}$), both beams have moved by about 2 μm, which is the maximum allowable distance the lower beam can travel. Consequently, in both cases the tuning range of the varactor can be designed to be very high and is limited only by fabrication issues, such as residual stress, thickness and roughness of the dielectric layer.

III. Fabrication Process

Fig. 2 summarizes the six-mask process that is necessary for the fabrication of the varactor. The varactors are fabricated on a high-resistivity Silicon substrate (approximately 2000 Ω-cm) with 2000 $\AA$ of thermally grown SiO_2. The fabrication starts with a lift-off process of Cr/Au 250/9000 $\AA$ that is performed to define the 50/80/50 cpw lines and the actuation pads. PECVD deposition of 3000 $\AA$ Si_3N_4 follows, which is patterned with a dry RIE process. This dielectric layer is mainly deposited to protect the actuation pads from potential direct contact with the upper beam. The first sacrificial layer (photoresist SC1827 by Shipley) is subsequently spun at 3.5krpm and patterned. This sacrificial layer is post-baked at a 180-C hotplate for 3.5 min to avoid any out-gasing in the remaining of the process. The lower beam deposition and patterning follows. This beam is made of low-stress 0.7 μm Au and is anchored at two or four points, depending on the design (see Fig. 1). A second sacrificial layer (photoresist AZ 9260 by Clariant) is spun at 3krpm and patterned. This photoresist results in a 6-μm layer after being post-baked in a 150-C oven for 1h. A thin layer (1000 $\AA$) of low-stress Au is subsequently sputter deposited on top of the second sacrificial layer. This layer is electroplated to 12-13 μm to create the very stiff upper beam described in Section II. The final steps are the etching of the sacrificial layer and drying of the varactors with a conventional supercritical CO_2 process. It is worth noting that no adhesion layer is required between the sputtered Au and the photoresist in both depositions described in this process. Such an adhesion layer (e.g. Ti or Cr) could easily create a significant mismatch between the two metals (Ti/Au or Cr/Au) and result in a significant warping of the structure.

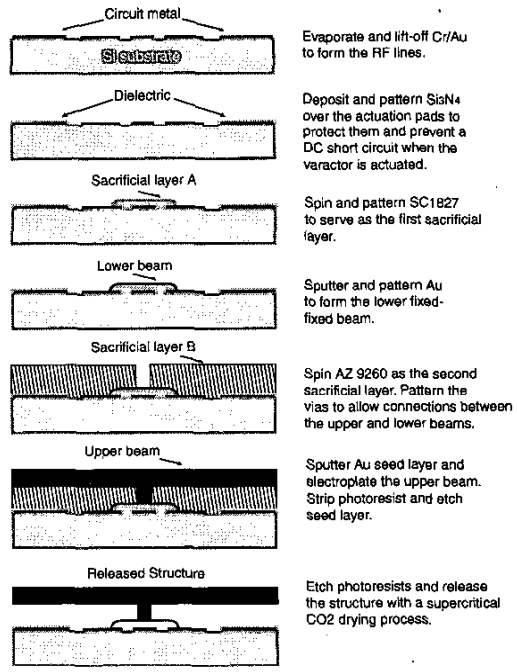

Fig. 2. Process flow for the fabrication of the proposed MEMS varactor.

IV. Results and Discussion

A. FSLB Tuning Range

The RF performance of these varactors was measured from 2-40 GHz by an 8510C Vector Network Analyzer with the help of an Alessi Probe Station and GGB Picoprobe 150 μm pitch coplanar probes. The effects of the probes and their RF lines to the network analyzer are de-embedded by a standard wideband TRL calibration. The RF shunt capacitance of each of the varactors was extracted by fitting the RF results to the model shown in Fig. 3c. Fig. 3a presents the measured reflection coefficient of a typical varactor following the geometry of Fig. 1b. These measurements prove the almost ideal capacitive response of the varactor for the various bias voltages. The capacitance, however, does not vary smoothly with voltage, but it shows a deviation from the theoretically expected curve at bias voltages of 22-23 V. This intermediate discontinuity becomes more obvious in Fig. 3b where the extracted capacitance is plotted as a function of voltage. Varactor C in this plot is the varactor whose results are shown in Fig. 3a, while the three other curves represent the extracted capacitances from three more varactors with the same geometry.

Fig. 3 clearly demonstrates that the tuning range for all varactors is between 160-213% and the maximum and minimum capacitance values do not vary more than 12% and 20% respectively. Table I summarizes these results and

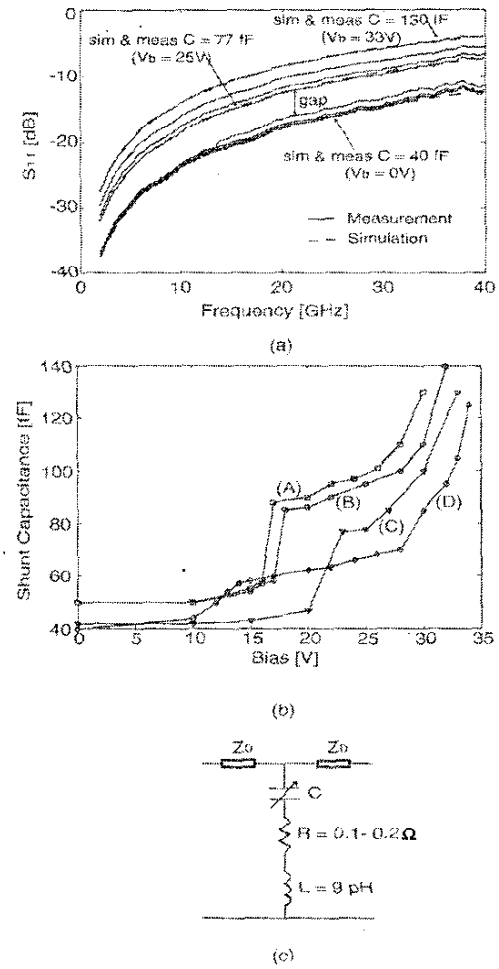

Fig. 3. (a) Typical measured and simulated reflection coefficient of the varactor shown in Fig. 1b. (b) Shunt capacitance presented by several varactors as a function of the applied bias voltage. Varactor C is the varactor whose reflection measurements are shown in the first part of this figure. It is interesting to note the discontinuity for each varactor that occurs at different voltage levels. (c) Equivalent circuit used to extract the capacitance values vs. bias voltage.

also provides the measured pull-in voltage and respective capacitance for each one of these varactors. This table shows that the maximum possible capacitance could not be achieved in an analog way. This was due to the residual stress in the lower beam that forced it to warp upwards and thus increase g_1, g_2 and therefore decrease $(g_2 - g_1)/g_1$. It is worth noting, however, that although the maximum tuning range could not be achieved because of residual stress, the device still demonstrated a significantly improved tuning range compared to previous designs.

It is also worth noting that the intermediate discontinuity was observed for all varactors but at different voltage levels. Fig. 3b shows that the voltage level where this discontinuity is observed varies by about 50%. Due to this effect it will be very difficult to realize some capacitance values close to the discontinuity region. Varactor C, for

TABLE I

SUMMARIZED RESULTS FOR THE VARACTORS PRESENTED IN FIG. 3.

Varactor	A	B	C	D
Min. measured cap. value (fF)	50	51	42	40
Max. measured cap. value (fF)	130	140	130	125
Pull-in voltage (V) (± 1 V)	31	33	34	34
Pull-in capacitance (fF)	270	265	230	240
Measured tuning range (%)	160	175	210	213

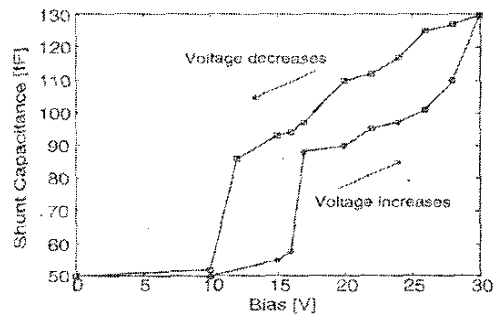

Fig. 4. Hysteresis loop for varactor A when the bias voltage is increased from zero to a value close to the pull-in voltage and is subsequently decreased back to zero.

instance, cannot easily provide the values from 47 to 77 fF. More studies need to be performed to explain this effect, but it is believed that it is due to residual stress that causes an abrupt movement as the device moves downwards.

The measurements presented in Fig. 3 were performed by slowly increasing the biasing voltage from 0 V to a value slightly less than the pull-in voltage. The reverse measurements were performed by decreasing the voltage from its maximum value to 0 V. Fig. 4 shows an example of such a measurement for varactor A. This Figure shows that a hysteresis loop exists in the operation of the varactor and that the observed intermediate discontinuity is observed at different voltage levels in the forward and backward biasing schemes. This hysteresis loop is repeatable and very similar for all the varactors of Fig. 3. Although more investigation is necessary to explain this hysteresis loop, we believe that it is a direct result of the existence of the intermediate discontinuity.

B. FFLB Tuning Range

The measurements presented in the previous subsection were repeated for the FFLB varactors. The results were in general similar, but the achieved tuning range was higher and reached nearly 300%. This improved tuning range was due to the fact that the fixed-fixed lower beam did not significantly deflect due to the process residual stress as it was the case for the FSLB designs. As a result, the lower beam could move almost the total distance of $g_1 = 2\ \mu$m without collapsing due to the pull-in effect of the upper beam. In order to verify this, we did not include any dielectric layer between the lower beam and the center conductor of the cpw for the FFLB design. As a result, if the voltage was increased past the pull-in voltage, a direct metal contact

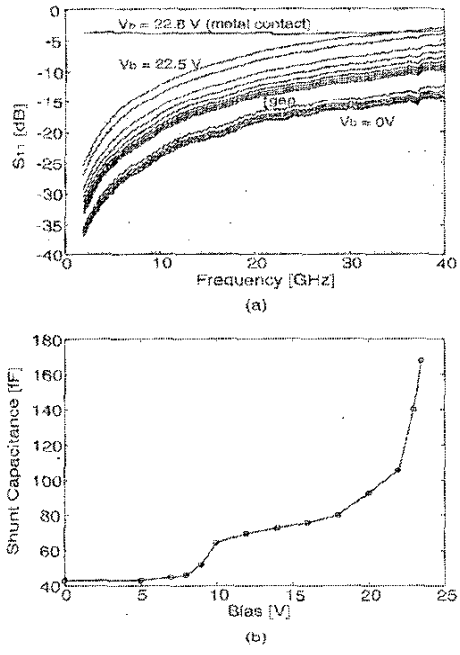

Fig. 5. (a) Typical measured reflection coefficient of the varactor showed in Fig. 1c. (b) Extracted shunt capacitance of the MEMS varactor as a function of the applied bias voltage. The tuning range of this capacitor is nearly 300%. Although the intermediate discontinuity is present in this varactor too, its effect is in general milder than the ones under the FSLB design.

would be observed and a low contact resistance would be recorded.

Fig. 5a presents the reflection coefficient measurements for a typical varactor of the geometry shown in Fig. 1c. The measurements demonstrate that the lower beam does not contact the center conductor of the cpw line even with a voltage of 22.5 V. However, when the voltage is increased to 22.8 V, a weak metal contact occurs, as the measured reflection coefficient at this biasing voltage indicates. The extracted capacitance values (except for $V_b = 22.8$ V) are presented in Fig. 5b. Based on the parallel plate model approximation, and these capacitance values, the gap between the lower beam and the center conductor at 22.5 V is approximately 0.36 μm. The fact that the upper beam does not collapse before the lower beam touches the cpw center conductor is also proven by the fact that the contact resistance can be precisely controlled by the bias voltage as shown in [6].

C. Resonant Frequency and Quality Factor

The resonant frequency of both FSLB and FFLB designs are very high and are dominated by the highest capacitance value and the parasitic inductance of the designs. The parasitic inductance depends on the springs of the lower beam and is in the order of 10 pH for both designs [6]. Consequently the resonant frequency of these varactors is very high (> 100 GHz) and could not be determined by the measurement techniques presented in this work.

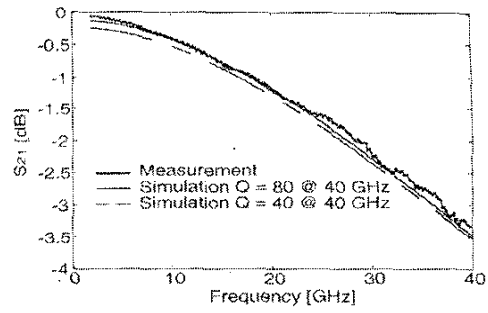

Fig. 6. Measured and simulated insertion loss of the varactor showed in Fig. 1c for $C = 168$ fF. The simulations were performed for various quality factors and two examples are presented in this Figure. These simulations indicate that the quality factor is at least 80 at 40 GHz.

The quality factor of these devices is also very high and is dominated by the resistive losses of the cpw line and the lower beam. Fig. 6 shows the insertion loss of a FFLB varactor with 168 fF capacitance and the simulated insertion loss for various quality factors at 40 GHz. This Figure demonstrates that the quality factor is higher than 80 at 40 GHz. More accurate quality factor measurement techniques will be presented in the conference.

V. Conclusions

In this paper we have presented a novel analog MEMS varactor design with a capacitance tuning ratio of 300%. The capacitance value is electronically controlled by a bias voltage which is in the range of 20-34 V. These MEMS varactors also show the additional advantages of resonant frequency and quality factor in excess of 100 GHz (for $C =$ 168 fF) and 80 at 40 GHz respectively.

Acknowledgments

This work has been supported by the Multifunctional Adaptive Radio, Radar and Sensors (MARRS) MURI project (award reference number 2001-0694-02).

References

[1] G. M. Rebeiz, J. B. Muldavin, "RF MEMS Switches and Switch Circuits," *IEEE Microwave Magazine*, vol. 2, pp. 59-71, Dec. 2001.

[2] C. L. Goldsmith, A. Malczewski, Z. J. Yao, S. Chen, J. Ehmke, and D. H. Hinzel, " RF MEMS Variable Capacitors for Tunable Filters," *Int. J. RF and Microwave CAE*, vol. 9, pp. 362-374, July 1999.

[3] J. Zou, C. Liu, and J. Schutt-Aine, "Development of a Wide Tuning-range Two-parallel-plate Tunable Capacitor for Integrated Wireless Communication Systems," *Int. J. RF and Microwave CAE*, vol. 11, pp.322-329, 2001.

[4] L. Dussopt and G. M. Rebeiz, "High-Q Millimeter-Wave MEMS Varactors: Extended Tuning Range and Discrete-Position Designs," *IEEE MTT-S Int. Microwave Symp. Dig.*, vol. 2, June 2002, pp. 1205-1208.

[5] J. J. Yao, S. Park, and . DeNatale, "High Tuning Ratio MEMS-based Tunable Capacitors for RF Communications Applications," *Solid-State Sensors and Actuators Workshop*, pp. 124-127, 1998.

[6] D. Peroulis and L. P. B. Katehi, "A Novel Device for In Situ Experimental Characterization and Reliability Analysis of DC-contact RF MEMS Switches," *submitted to the 12th Int. Conference on Solid-State Sensors, Actuators and Microsystems.*